
Response to Request for Additional Information – ANP-10268P
“U.S. EPR Severe Accident Evaluation Topical Report” (TAC No. MD3803)

RAI 1: Section 2.1.1.1, Figure 2-1:

The figure shows an irradiation capsule basket at the periphery, evidently outside the heavy reflector. Please describe the design and contents of this reflector, being sure to mention the structural materials used and what its contents would be. Describe how the basket and its contents would participate in the severe accident progression and in source term evaluations. Were these modeled in the MAAP 4.0.7 analyses? If so, how did they impact core debris and radionuclide inventories? If not, please provide a qualitative discussion of their impacts.

Response 1:

The irradiation capsule baskets participate in the Reactor Pressure Vessel Irradiation Surveillance Program (RVSP) for the U.S. EPR. The purpose of the RVSP is to monitor the changes of the mechanical properties of the reactor vessel ferritic steel in the beltline region due to the thermal environment and neutron irradiation. This is done by placing reactor vessel material samples, neutron dosimeters, and temperature monitors in capsules. The irradiation capsules are placed in irradiation specimen guide baskets. The specimen guide baskets are attached in the downcomer region on the outside of the core barrel at the mid elevation of the core. The specimen guide baskets and capsules are fabricated from a corrosion resistant material, such as stainless steel (i.e., SS304).

The irradiation capsule basket was not included in the MAAP4 analyses. [

], neglecting this relative small structure is not expected to have a discernable impact on conclusions drawn from analyses.

RAI 2: Section 2.1.1.1:

What are the guide thimbles joined to the top and bottom nozzles of the fuel assemblies made of? How are they modeled in the accident progression? What are severe accident implications of including them?

Response 2:

The guide thimbles are made of M5™ material. MAAP4 does not have an allowance for M5™. Therefore as a simplification, M5™ is assumed to be 100% Zr in this model. [

] MAAP4 does not explicitly model this component; rather, the associated mass must be lumped with recognized component such as fuel cladding. In the accident progression the deterioration of the guide thimbles occur simultaneously with the

deterioration of the fuel portion of the core. Modeling the guide thimble mass increases the amount of metallic melt that will relocate to the reactor cavity and spreading compartment. The main impact of the additional Zr mass will be increased hydrogen generation; however, the larger mass would also be expected to take longer to stabilize.

RAI 3: Section 2.2.1:

It has been stated in presentations to the NRC Staff that the severe accident depressurization valves would be manually opened when the peak outlet gas temperature would reach 650°C. How long would it take to perform this action once the signal has been received? What are the existing procedures to assure that the action would be taken? How long a delay in performing this action (after the 650°C temperature is reached) can be tolerated before the hot leg, surge line, or steam generator tubes would be threatened by creep rupture?

Response 3:

While Section 2.2.1 does not provide information related to the use of the severe accident depressurization valves within a severe accident management strategy, information provided to the NRC in prior AREVA presentations has detailed the role of these valves in the manner described in this RAI. In fact, Section 6.4.1.1.6, which provides a description of the MAAP4.0.7 model used, states this assumption for the U.S. EPR severe accident analyses. Specifics related to a severe accident management guidelines and strategy for the U.S. EPR will be addressed during detailed design. Nonetheless, analyses prepared for the U.S. EPR design certification have assumed that the operator reliably begins RCS depressurization when the core outlet temperature reaches 650 °C (1200 °F).

Uncertainty associated with the required operator action is explicitly treated in performance analyses supporting the application of MAAP 4.0.7. [

] The inclusion of this extended period of core damage before depressurization was chosen as a means to encourage hydrogen generation to meet 10 CFR 50.44 requirements. Nonetheless, results from the uncertainty analysis could be used to infer a grace period for this action within a severe accident management strategy. In fact, the MAAP4.0.7 model also considers the potential for creep rupture of steam generator tubes, hot leg, or the surge line. As such, not only is the capability to consider these uncertainties being addressed as part of safety issue resolution, results from this uncertainty analysis are applicable to the decision-making activities that will be required as part of the tasks associated with detailed design.

RAI 4: Section 2.2.1:

The last paragraph provides discussion on the positive contribution of Pressurizer Relief Tank (PRT) rupture disks in promoting mixing of steam, hydrogen and non-condensable gases in the RCP rooms. However, there is no discussion provided either in this section or under combustible gas control section, on the potential for hydrogen stratification due to jets and/or plumes forming in this area following PRT rupture disk actuation. In addition, please discuss the

role of PRT in hydrogen distribution for scenarios where vessel is depressurized and the RPT is failed well before core damage and significant hydrogen production.

Response 4:

Density-driven hydrogen stratification cannot occur in the RCP/SG rooms because the natural convection that takes place in those compartments during an accident is independent of PRT discharge. Compartment pressurization (i.e., breaks or PRT discharge), temperature differences between compartments, steam condensation on cold surfaces, recombiners and the hydrogen mixing system (i.e., series of convection and rupture foils and mixing dampers) play a significant role in stimulating atmospheric mixing and convection. When the PRT rupture disc fails, the contents are discharged in the RCP/SG compartments; this process enhances mixing and convection. The PRT contents are discharged in the direction of the floor of the RCP/SG compartments (perpendicular to the floor). In the case of a high energy release, the jet released from the PRT would be deflected by the floor and dissipate the plume concentration. In the case in which the RCS has depressurized prior to core damage, the PRT has essentially no role in hydrogen dispersion; however, at low pressure hydrogen delivery and distribution in the containment would be slower and at a pace which could be adequately controlled by the system of PARs and the hydrogen mixing system.

RAI 5: Section 2.2.2.2:

It is stated that, in the event of an accident, communication would be established among equipment rooms to eliminate potential dead end compartments where non-condensable gases could accumulate. What is the likelihood of communication not being sufficiently established, and what would be the consequences of this?

Response 5:

In the main equipment rooms (SG/RCP), where the hydrogen is discharged, there are no physical barriers to prevent connectivity. For global convection, the hydrogen mixing system is designed to reliably respond to pressure and temperature disparities between the inner regions of the containment immediately surrounding the RCS and outer expansive region. This is accomplished via opening of rupture and convection foils in the SG ceiling and mixing dampers adjacent to the air space above the IRWST. Therefore, the formation of pockets containing reactive gas mixtures is prevented for the suite of relevant scenarios.

The principal objective related to the containment transformation into a single convective volume is to enhance the mixing of air, steam, and hydrogen within the containment atmosphere to minimize the potential for a combustion event. Without "sufficient" mixing, the full benefit of the suite of PARs external to the inner containment area would not then be realized. Given that PAR performance is a function of hydrogen concentration, overall hydrogen removal capability would not be diminished proportionally to the number available. Uncertainty associated with the area opened between the inner and outer containment during a severe accident is explicitly addressed in the uncertainty analysis being prepared for the DCD.

RAI 6: Section 2.2.3.1:

It is stated that the high iron oxide content of the reactor cavity concrete promotes oxidation of the remaining zirconium and uranium within the melt, before the zirconium bricks would be attacked. How high does the melt temperature increase from this oxidation, and why doesn't this temperature increase lead to a higher melt temperature for spreading?

Response 6:

While the oxidation of metals within the core melt will add energy to the mixture, a significant amount of energy is lost through the decomposition of concrete and, to a lesser extent, thermal radiation to the reactor cavity environment. Calculation results show that there is a small difference in melt temperature between the time of reactor vessel failure and gate failure; however, the effects of the different heat transfer mechanisms do appear in between those times. Since the resident metals within the core melt oxidize at a rate proportional to the supply of concrete decomposition products, the impact on corium temperature is visible during the early portion of the retention phase. As the Zr and U metals are depleted, the dominant concrete decomposition products (iron oxide and silica) start to accumulate in the melt, lower the liquidus temperature and consequently, the melt temperature. Additional contributors to the temperature decrease are the heat loss due to concrete decomposition and thermal radiation. As shown in Figure RAI-6-1 (a revised calculation result for the SBLOCA case provided in the topical), the contributions of these primary heat transfer mechanisms appear to essentially offset one another. Specifically, Figure RAI-6-1—Reactor Cavity Corium Temperature Response, illustrates the temperature response of the corium in the reactor cavity.

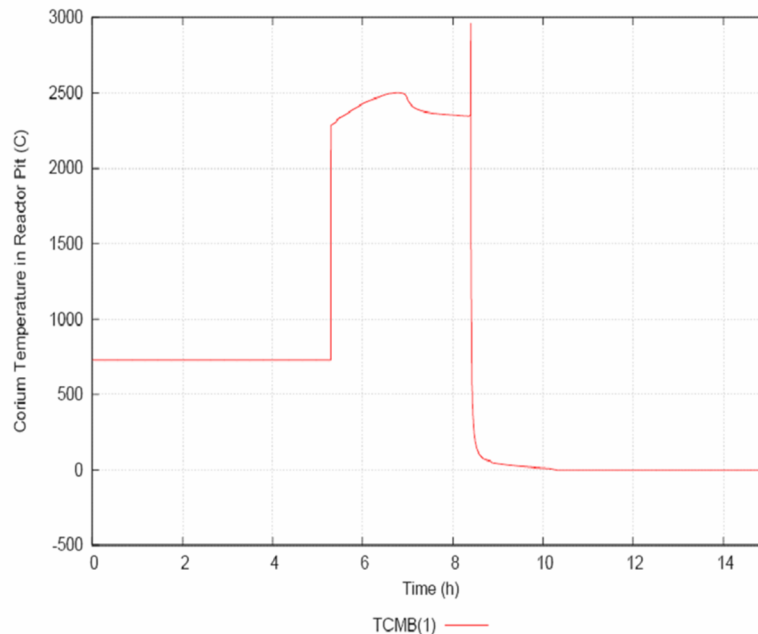


Figure RAI-6-1 Reactor Cavity Corium Temperature Response

Note: the temperature spike at the time of gate failure is the result of a numerical anomaly and has no physical basis.

RAI 7: Section 2.2.3.1:

Please describe how the formation of silicates would lower the radionuclide release from the corium pool. What are the chemical reactions and the resulting vapor pressures of radioactive species?

Response 7:

The confirmation that the MCCI has a strong positive effect on the retention of the low-volatile fission products, like Sr, Ba, La, etc. was a key outcome of the ACE program, performed at the Argonne National Laboratory. It was also confirmed by later analysis with thermo-chemical codes, like SOLGASMIX. Corresponding results were reported during the 2nd OECD (NEA) CSNI Specialists Meeting on Molten Core Debris-Concrete Interactions, April 1992.

Fission product immobilization by MCCI is attributed to the formation of silicates, carbonates and zirconates that starts after Zr-oxidation and becomes effective already at low fractions of added concrete. A precise general prediction of radioactive species and vapor pressures is not possible as they depend on melt composition, temperature and ambient conditions (containment atmosphere). Analyses with MAAP4.0.7 do not credit this phenomenon.

RAI 8: Section 2.2.3.4:

It is stated that the cooling elements would be flooded with water from the IRWST prior to initial contact between them and the core debris. Is this flooding done automatically? If not, what alerts the operator to initiate the action, and how much time would elapse from initiation of the signal to the flooding?

Response 8:

Flooding of the cooling structure is based on the melting of thermally sensitive initiators, consisting of a material of low melting point, installed on the floor of the spreading area. When the initiator is destroyed during contact with molten core debris, the spring loaded actuator of the flooding valve will be allowed to open and water will flow from the IRWST. This process is entirely passive and does not depend on or require operator action. The flooding valve is strictly passive and is not controlled by operator action. (see also RAI 9 response)

RAI 9: Section 2.2.3.4:

More information on the operation and location of the two spring loaded flooding valves would be required during design certification application. Is it possible that flooding valves fail prematurely thus arresting the melt spreading? Under what conditions (partial spreading, non-uniform spreading) is it possible for the flooding valves not to open? Also, is this flooding valve actuation passive, or can the operators manually open the valve and start flooding? What are the potential implications of any fuel-coolant-interactions, if delayed release of some core debris (i.e., due to the late melting and relocation of remaining fuel inside the damaged core after cavity plug melt-through) could pour into the already flooded initial melt pool in the spreading room?

Response 9:

Each of the two passive flooding valves is located in a dedicated compartment adjacent to the spreading area (refer to Figure 2-21 of the Topical Report). A metallic cable is connected from the valve actuator to a thermally sensitive initiator installed on the sacrificial concrete in the spreading area. When the valve is in the closed position, the cable is maintained taut by the force applied to compensate the spring tension of the valve actuator. The valve will remain closed as long as the cable is taut. The function of the cable is to communicate the melting of the initiator to the passive flooding valve. The tension of the cable and its direction changes are ensured by pulleys anchored to the ceiling and the walls. In order to avoid an inadvertent opening of the valves due to rope fatigue, thermal expansions, or earthquake accelerations, a spring is integrated in each cable to compensate for changes in the length (for an overview of the flooding valve actuation and arrangement refer to Figure 2-22 in the Topical Report).

Melting of the thermal initiators is triggered by the arrival of corium melt at a temperature in the range of 1500 to 1600 °C. The material to be used for the initiator will be identified during the detailed design phase for the U.S. EPR; however, it is expected to have a melting point within the range of 250 °C – 1000 °C. Once the initiator is molten, the cable is relaxed and the force of the spring in the valve actuator is released and thus opens the flooding valve. No electrical power or operator action is required for the passive flooding valves to operate. The operator has no way to affect the valves' performance either by remote signal or manual operation. The ambient conditions during a severe accident are such that no access to the flooding valve compartments is possible to manually operate those valves.

The operation of the passive flooding valves is based on the arrival of corium on the spreading area destroying the thermal initiators. Failure to open or a premature opening of the passive flooding valves is unlikely. Partial or non-uniform spreading is practically eliminated through the melt retention and conditioning phase that occurs in the reactor cavity. The principal objectives of that phase in the U.S. EPR severe accident progression are to maximize the collection of molten corium and condition the melt to be conducive to spreading.

The destruction of the initiators will likely occur prior to complete melt spreading. However, at least 3 – 5 minutes will pass by before water will start to overflow from the cooling structure thus providing more time for the molten corium to spread and settle. [

] Also, water overflow from the cooling structure onto the melt will only occur along the side walls perpendicular to the main cooling channel far away from the transfer channel. At least an hour is expected to pass before the entire cooling structure is flooded to overflow level and the relevant water level in the spreading compartment increases again as IRWST water level continues to drop.

Several conditions are expected to exist to reduce the likelihood of FCI. Foremost is that the state of the melt benefits from the retention and conditioning that occurs in the reactor cavity. This improves the viscous character of the oxidic melt on top. In addition, the sidewall delivery of coolant, the low flooding rate, and the large spreading area minimizes energetic reactions by lowering the surface heat flux and focusing a limited amount of water at the boundary of the melt. Early crust formation serves as a protective layer against water contact with the more reactive liquid melt, while ongoing MCCI creates fissures in the crust that enhance the cooling effect of the over-layer of water. Other conditions that inhibit FCI are the higher containment pressure and low water subcooling. Experimental evidence from spreading and pouring tests in wet conditions such as MACE, CORINE, FARO, RIT, and KATS test support the premise that

FCI is not a concern. See RAI 27 response for additional discussion of the flooding process.

RAI 10: Section 2.2.4.1:

It is stated that cooling the debris would release steam that would pressurize the containment, and that containment design pressure would not be reached for several hours following the onset of core damage. How long would it take before containment failure pressure would be reached? Is venting a possibility? If so, would the release be scrubbed?

Response 10:

Analysis to evaluate containment ultimate pressure will be evaluated for the DCD. As a rule-of-thumb, ultimate or failure pressure is between 2 – 2.5 times design pressure. Design pressure is about 5.3 bar (abs). Assuming an ultimate pressure of twice design pressure (10.5 bar) and that the Severe Accident Heat Removal System has failed, then linearly projecting the pressure rise shown in Figure 7-14 of the topical, ultimate pressure would be reached around the 72nd hour. While venting and scrubbing are possible with the U.S. EPR design, development of the specifics related to a severe accident management strategy will be addressed during detailed design.

RAI 11: Section 2.2.4.2:

What is the likelihood of core debris particles causing flow blockages in the heat exchanger and causing failure to deliver condensate water to the containment sprays?

Response 11:

Section 2.2.4.2 describes the Severe Accident Heat Removal System. The debris implied in that description includes such items as loose parts and building/equipment fragments. A sufficient degree of separation between the IRWST and the reactor vessel, reactor cavity, and spreading compartment exists such that the possibility of core debris entering the IRWST is precluded.

The possibility of a flow blockage resulting from debris has been considered in the design of the IRWST. The SAHRS system includes a strainer to prevent debris from collecting downstream in the SAHRS system, where maintenance to address such a blockage would be more difficult. In addition, to limit the transport of debris that could clog the SAHRS strainer, a back flushing line is used to remove the debris bed from the screen. The back-flushing of the SAHRS screen is achieved by injecting water with the SAHRS pump taking suction from the SIS sump screen of the neighboring SIS train. These measures resulting in reliable SAHRS performance have been credited in the analysis of credible severe accidents for safety issue resolution.

RAI 12: Section 4.1:

Page 4-2 of the topical report states that "containment bypass mode is addressed through preventive features." It is recognized that the placement of IRWST inside containment minimizes the traditional "event V" frequency. However, it is not clear how the issue of steam generator tube rupture (i.e., as accident initiators and/or induced by conditions of the accident) can be eliminated through preventive measures. Please elaborate.

Response 12:

In the "Reactor Safety Study," (WASH-1400), published in 1975, and in NUREG-1150, "Severe Accident Risks: An Assessment for Five U.S. Nuclear Power Plants," the NRC described the intersystem loss-of-coolant-accident (ISLOCA) outside containment as an event of low core damage frequency, but as one of the main contributors to plant risk. In those studies the NRC referred to the ISLOCA as "Event-V." Most probabilistic risk assessments (PRA) have also shown that the ISLOCA is very unlikely. Similarly, preliminary Level 1 PRA for the U.S. EPR also results in a low core damage risk resulting from an ISLOCA ($< 10^{-8}$). As such, this particular event is not included in evaluating the breadth of possible end states impacting the U.S. EPR's severe accident mitigation features (i.e., hydrogen control, core debris stabilization, containment performance, high pressure melt ejection, and equipment survivability).

Due to the strategy to depressurize the RCS with a dedicated system with high capacity together with other measures, e.g. to avoid violent hydrogen deflagration, the likelihood of early containment failure is low. Other sequences, such as sequences with containment bypass or with open containment can also lead to early large release. Despite their practical elimination they are considered for their potentially large consequences in PRA. The SGTR is an important contributor to containment bypass, both as initiating event and induced by hot gases or dispersed melt particles. The major contribution here is related with overfilling of the SG secondary side and failure of the operator to fully depressurize the RCS. In this case, fission products leaving the containment have to pass through the secondary water leading to efficient retention.

SGTR as a consequence of core melt, on the other hand, is unlikely due to high reliability of depressurization of the RCS. The high degree of leaktightness of Main Steam Isolation Valves, with the control of sealing surface, guarantee that residual leaks in case of SGTR core melt scenario are consistent with radiological targets.

Nonetheless, the SGTR is a plant damage end state that can be modeled with MAAP 4.0.7 such that results can be used in a PRA Level 3 evaluation.

RAI 13: Section 4.2.1:

The core support plate and core reflector represent more massive structures than in current LWRs. These structures may tend to remain in the RPV, potentially restricting the transport of molten core material to the reactor cavity after vessel breach, or they may become part of the core debris exiting the vessel. Discuss how these structures are treated in the analysis of core melt progression, and how the quantity of core debris mass exiting the RPV is assessed. How does this debris participate in potential direct containment heating (DCH) events (for high RPV pressure scenarios), core debris-concrete interactions, and hydrogen production both in-vessel and ex-vessel.

Response 13:

As conveyed in the RAI, the U.S. EPR design differs from the core designs of current generation LWRs. Specifically, current generation LWRs have a core region surrounded by a water baffle region contained within the core barrel. The configuration for the U.S. EPR has the heavy reflector and core barrel immediately surrounding the core with no bypass region. With the implementation of the thicker lower core support plate and heavy reflector coupled with the elimination of the bypass region, the melt progression into the lower plenum is subsequently delayed due to the greater thickness of the radial boundary.

MAAP4.0.7 contains models to address the in-vessel melt progression described in Section 4.2.1 of the topical report. Most of these models are retained from earlier versions of MAAP4 and are described for the HEATUP subroutine in the MAAP4 users' manual. To address the in-vessel progression phenomena unique to the U.S. EPR, MAAP4.0.7 was revised to explicitly consider the unique heavy reflector/core barrel configuration described above.

MAAP4.0.7 is capable of tracking the two core melt pools that evolve within the core and the lower plenum. This includes the processes that result in the failure of the upper portion of the heavy reflector, thus providing a flow path from the core to the lower plenum. Simultaneously, MAAP4 models core melt relocation downward toward the lower core support plate, considering the impact on melt state resulting from heat transfer to existing structure, the formation and dissolution of blockages, and the ongoing metal-water reaction. MAAP4 will then predict contact between the lower core support plate and the melt which will exacerbate the erosion of this component. Erosion and subsequent failure of the component is driven by the amount of energy transferred from the core melt. The rate of component failure is a function of several parameters and, as such, the timing of lower core support plate failure relative to reactor vessel failure is highly uncertain. As a consequence, the amount of core melt in the lower head available to relocate to the reactor cavity during the initial pour is sensitive to the prior in-vessel progression predicted by MAAP4.

An important element of the initial reactor cavity response is the extent of molten debris which drains from the failed reactor vessel lower head. MAAP4.0.7 does include a revision to simulate the expected dynamics for reactor vessel failure originating near the upper part of the melt-contacted region in the lower plenum. The model is drawn from results demonstrated in several experiments, including COPO/COPO-II, FOREVER and Sandia National Laboratory's LHF programs. The actual amount of relocated melt will depend on the achieved completeness of melt relocation from the upper pool into the lower head. If the lower support plate had already failed, it is conceivable that the entire core inventory could become relocated into the lower pool at that time. Among the constituent elements of the melt will be metals and oxides from the core, support structure (including the lower core support plate), heavy reflector, and the lower head.

For the reactor cavity region, MAAP4.0.7 includes heat transfer models to address the dominant heat transfer mechanisms present during MCCI. The heat transfer rate between core melt and concrete can either be modeled applying user defined values or using an experimentally-based empirical model. Heat transfer from the core melt to the concrete is applied to the decomposition of concrete modeled to consider the common chemical reactions anticipated. Energy and chemical composition is tracked to ensure melt properties are accurately predicted. Among the chemical constituents tracked within MAAP 4.0.7 is hydrogen which is assumed to be released into the adjoining containment compartment. In addition, MAAP4.0.7 was upgraded so that heterogeneous structures in the containment could be modeled such as the presence of

sacrificial concrete over a ceramic protective layer.

When considering the many uncertainties associated with in-vessel progression, the breadth of possible release sequences is large. This fact was the primary motivation of the melt retention and conditioning feature in the U.S. EPR. With the temporary melt retention and melt condition phase, the validation of this concept does not rely on certain release sequences as calculated with codes like MAAP4.0.7. Rather, it is based on an integral method which supports itself on simple energy-balance considerations. Demonstration of this capability will be prepared to support content in the DCD.

With regard to high pressure melt ejection and subsequent DCH, MAAP4.0.7 does include models to consider these phenomena. Analyses performed for safety issue resolution credits the manual system depressurization planned for severe accident management as described in Section 5.3 of the severe accident topical report. As such, DCH does not occur in these credible severe accident scenarios. Presentation of the likely plant damage end states that influence the potential for high pressure melt ejection and subsequent DCH will be further developed in the DCD.

RAI 14: Section 4.2.1:

What model parameters are relevant in the MAAP treatment of the evolution of the two molten pools and multiple pours into the cavity? Please describe any sensitivity studies that include variations of these parameters. Of particular interest would be vessel failure timing, amount and time-dependent temperature of core debris entering the cavity, and any impacts on containment failure time.

Response 14:

Related to the safety issues of interest, i.e., hydrogen control, core debris coolability, and containment overpressurization, are several factors that can influence the progression of a severe accident. Uncertainties related to both scenario progressions, including scenario type, and physical processes impacting event progression are to be considered for analyses to be presented in the DCD. Code inputs well-correlated to one of these principal safety issues have been identified and their corresponding uncertainty ranges have been defined. The basis for the identified parameters is founded in several Phenomena Identification and Ranking Tables (PIRT) appearing in the literature for severe accidents, matched to the principal phenomena of interest for the U.S. EPR presented in Table 4-2 of the Severe Accident Evaluation topical report. This is given in Table RAI-14-1 below. The phenomena of interest in Table RAI-14-1 are further characterized and mapped to code input parameters in Table RAI-14-2 in Response 14 of this document. Table RAI-14-2 also includes the recommended uncertainty ranges. These are based on FAI experience. Some of these parameters are biased to address the 10 CFR 50.44 requirement that combustible gas control system performance analysis consider the hydrogen generation from 100% clad-water reaction. The uncertainty parameters presented here do not include those MAAP4 parameters assigned in the base U.S. EPR model with values considered bounding. While those parameters may be significant contributors to event progression, using bounding values addresses the uncertainty concern. In most instances the probability distribution functions are assumed to be uniform.

Among the analyses being performed to provide insight into the performance of the U.S. EPR's severe accident features will be a Monte Carlo-style uncertainty analysis for which each of the

identified uncertainty parameters will be sampled. The result of this analysis will provide several key measures relating the anticipated tolerances of the design, including “vessel failure timing, amount and time-dependent temperature of core debris entering the cavity, and any impacts on containment failure time.” Results from this analysis will be conveyed in the DCD.

Table RAI-14-1 Mapping of Identified Phenomena to MAAP4 Model

Phenomena Class	Associated Phenomena	Model Implementation Description
1. Thermal-hydraulic and fuel rod degradation	Stored energy	Total Power
	Decay Heat	
	Zr-Steam Oxidation Parameters	Zr-H ₂ O Oxidation Multiplier
2. Core melt progression	Zr melt breakout temperature	Cladding Integrity with Oxidation
		Cladding Creep Rupture Temperature
	Fuel rod collapse temperature	Material Creep (Larson-Miller) Limit
	Fractional local dissolution of UO ₂ in molten Zr	Contact Area Multiplier
	Core material melt temperatures	Fuel Melt Temperature
Control Rod Melt Temperature		
3. Core melt relocation to lower head	Melt relocation heat transfer coefficient	Flow blockage based on porosity
4. In-vessel fuel coolant interaction	Addressed independent of uncertainty analysis (see Assumptions)	
5. In-vessel oxide/metal separation	Function of oxidation process and relocation, see #1, #2 and #3	
6. Crust formation and failure	Gap heat transfer	Conservatively neglected
7. In-vessel debris formation	Heat Transfer within fuel debris beds	Particulate debris size and debris porosity in lower plenum
8. RPV failure modes	Local and Global Lower Head/Vessel Failure	Initial radius of the local vessel failure
		Lower head damage fraction for failure
		corium friction coefficient (in contact with vessel following failure)

Phenomena Class	Associated Phenomena	Model Implementation Description
	Thermal radiation exchange	Emissivities
9. Melt conditioning in reactor cavity	MCCI integrity of ex-vessel protective structure	Downward heat transfer coefficient
		Side wall heat transfer coefficient
		Flat Plate CHF Kutateladze #
10. Melt spreading in spreading compartment	Ablation of melt plug and gate	Melt plug geometry
	Other aspects addressed independently of uncertainty analysis	
11. MCCI in spreading compartment	MCCI	See #9
12. Spreading compartment flooding and basemat cooling	Decay heat MCCI	See #1 and #9
13. Steam/hydrogen transport	Containment transition to single convective volume	Flow area between containment compartments
14. Hydrogen recombination	PAR efficiency	Rate of recombination
		Operation cutoff based on H2 concentration
15. Hydrogen combustion	Auto-ignition temperature	Local/Global
16. Long-term containment heat removal	Will be addressed independent of uncertainty analysis	
17. Fission product transport	Will be addressed independent of uncertainty analysis	

Table RAI-14-2 Summary of Parameter Ranges for Uncertainty Analysis

Parameter	Description	Low Value	High Value
HYDROGEN UNCERTAINTY PARAMETERS			
FAOX	Zr-H ₂ O Oxidation Multiplier	1.5	2.0
FZORUP	fraction of Zr oxidized to keep cladding intact	0.0	NA
TCLMAX	Cladding Melt Breakout Temperature	2500 K	3000 K
LMCOL	Fuel Rod Collapse Temperature	46	54
IEUTEC	enable/disable the U-Zr-O eutectic model	NA	1
TEU	Fuel Melt Temperature	2500 K	2800 K
TEUBS	Control Rod Melt Temperature	1500 K	2500 K
EPSCUT/EPSCU2	Melt relocation HTC	0.0	0.15
XDJETO	Particulate debris size in lower plenum	0.01	0.1
EPSPB	Porosity of fuel debris beds	0.26	0.53
TJBRN	Local auto-ignition temperature	NA	3000 K
TAUTO	Global Auto-ignition temperature	NA	3000 K
CORE DEBRIS COOLABILITY UNCERTAINTY PARAMETERS			
QCR0	Total Power (decay power)	4.59E9	4.8654E9 (6% high ~2sigma decay heat)
XROF0	Initial radius of the local vessel failure	0.005 m	0.25 m
FDAMLH	Lower head damage fraction for failure	0	1
FRCOEF	corium friction coefficient	0.001	0.1
FCHF* (max)	Flat Plate CHF Kutateladze #	0.2	0.3

Parameter	Description	Low Value	High Value
FCHF* (steaming rate)	Steaming rate (kg/s)		
EWL, EEQ, ECM	Emissivities		
TRANSIENT UNCERTAINTY PARAMETERS*			
TDPOWR (ATWS only)	Scram Power Ramp-Down Delay		
ABB (Seal LOCA only)	Break Area (Diameter, in)		
ABB (Pipe Break LOCA only)	Break Area (Diameter, in)		
PSGRV	SG MSRV (broken loop only)		
User defined**	SADV signal on T(COROUT)		
User defined	SADV actuation delay		
FEFPAR	PAR capacity scale factor		
NFH2MN	PAR Threshold for operation		
PFFJ or PFBJ	Failure pressure		
AJUNC0*	Junction Area		

RAI 15: Section 4.2.1:

The picture conjectured for the U.S. EPR core melt progression for the phenomenologically-bounding severe accident assumes that the in-core molten pool will have to extend to the heavy reflector and/or the heavy core support plate before it relocates downwards. Please elaborate why this is considered to be bounding. For example, why exclude a scenario that will involve the formation of metallic blockages in the lower region of the core (but well above the core support plate) initially supporting the in-core melt crucible, then followed by side failure of the crucible prior to reaching the heavy metal reflector? In addition, what is the justification for assuming the core support plate to remain intact if a substantial quantity of molten debris is residing above it? What is the time-to-failure for core support plate under substantial loading conditions (heavy mass at high temperature) of severe accidents?

Response 15:

The presentation of the “phenomenologically-bounding severe accident” was made to highlight the phenomena and processes apparent as the event progresses to lead into the identification of the key phenomena and processes given in Table 4-2 of the topical. The provided description does not preclude various permutations to in-vessel progression such as the one described in the RAI. Nonetheless, the “phenomenologically-bounding severe accident” describes a scenario in which heat transfer in the core is significantly degraded, thus core/corium temperatures are maximized. Failure of the heavy reflector provides a convenient path to move corium to the lower head early in the event (when decay heat is the highest), thus beginning the thermo-chemical attack on the lower head. A large, early core melt release to the reactor cavity is bounding for core melt stabilization since decay heat is high and melt temperatures would also likely be maximized. Higher temperatures can also be considered a bounding condition for containment performance following flooding of the melt with regard to containment overpressurization from the generation of steam in the spreading compartment. With regard to hydrogen generation, there is no unique event characteristic for maximizing clad-water reaction other than to ensure a sufficient amount of reactants in contact with each other at high temperature.

As described in RAI response 14, MAAP4.0.7 will predict failure of the lower core support plate based on the code’s inherent heat transfer modeling and loading. There is no intention to assume any non-physical behavior in the description provided in Section 4.2.1 of the topical. The analysis results and related uncertainties considered (including in-vessel phenomenological and process uncertainties) associated with melt relocation from the reactor vessel to the reactor cavity will be conveyed in DCD.

RAI 16: Section 4.2.1:

Although high-pressure scenarios are much less likely than scenarios where the RPV is depressurized, DCH loads and ex-vessel fuel-coolant interactions should still be quantified for the U.S. EPR. Please discuss the magnitude and consequences of these loads for high-pressure scenarios.

Response 16:

As stated in Section 5.3 of the topical report, HPME and associated DCH are not considered credible severe accident phenomena for the U.S. EPR. The U.S. EPR design includes features that make the risk from HPME negligible. The key feature is the primary depressurization system; however, low core power density, a RPV lower head without penetrations and a torturous pathway from the reactor cavity to the upper containment contribute to preventing or mitigating the potential consequences of high pressure melt ejection.

As remote phenomena for severe accidents, HPME and subsequent DCH are not examined using the MAAP4.0.7 code. Rather, an analytical method based on NUREG/CR-6338 and FZK report FZKA 6988 is employed to generate a bounding result for the consequences of these phenomena. This method is a strong function of the RCS pressure at the time of RPV failure. MAAP4.0.7 calculations are used to support the inputs for this approach. The results of this analytical approach will appear in the U.S. EPR DCD. As stated in the response for RAI 13, presentation of the likely plant damage end states that influence the potential for high pressure melt ejection and subsequent DCH will be further developed in the DCD.

RAI 17: Section 4.2.1:

What are the potential implications of Reactor Pressure Vessel (RPV) lower head failure at high pressure? What is the maximum displacement of the RPV for both "localized" and "hinged" failure modes? Please elaborate.

Response 17:

The U.S. EPR credits a highly reliable depressurization system to practically eliminate high pressure reactor vessel failure scenarios. Nonetheless, MAAP4 can be used to assess the possible impact of reactor vessel failure at high pressure. MAAP4 can provide key inputs for this analysis including RPV pressure and exit mass flow at the time of reactor vessel failure.

The weight of the RPV [] and restraining forces [] in combination can be shown to exceed the maximum calculated upwards thrust on the vessel by more than an order of magnitude. This will be further developed in the DCD.

RAI 18: Section 5.0:

Please provide a list of relevant experiments that were performed to test the unique features of U.S. EPR (include major findings and scalability issues), and the use of test data to validate analytical tools and models.

Response 18:

Section 5.0 identifies several test programs and major findings related to severe accident phenomena relevant to the (European) EPR. Several of these tests were specifically inspired

by the development of the EPR design. In particular, given the EPR's unique ex-vessel melt stabilization approach, most MCCI test programs reference the EPR as the motivation for investigation. In addition, tests on hydrogen recombiners and the basemat cooling structure are EPR-specific.

With the EPR, AREVA strives to maintain as much standardization as is possible. Design differences between the European product and the U.S. product do exist as a consequence of meeting the regulatory, design code, and economic constraints unique to the different regions. With regard to severe accident response features, very little has been changed. Given the consistency between the U.S. and European designs, no new tests were performed for the U.S. EPR.

RAI 19: Section 5.1.1.1.1:

How much hydrogen is produced from oxidation of the steel reflectors for the various accident scenarios considered?

Response 19:

MAAP4 does model the oxidation of steel and the subsequent release of hydrogen. The RAI 35 response provides further detail describing this capability. MAAP4 does not explicitly provide results on hydrogen generation from steel oxidation. It can be inferred from results for Zr oxidation. A survey of the analysis results being prepared for the DCD shows that up to 15% of the total hydrogen produced resulted from oxidation of steel.

Note: To obtain the 15% value the following method was applied:

From the root directory of the uncertainty analysis run:

$$\text{devplotmaap}'(\text{mh2cr} - (1512 * \text{fzrrc}) + 0.00001) / (\text{mh2cr} + 0.00001) * 100'$$

where: mh2cr is the integrated mass of hydrogen generated in the core (criterion),
fzrrc is the fraction of zirconium reacted on clad, and
the 1,512 (kg) is the amount of hydrogen that 100% of clad oxidation can create.
The 0.00001 values avoid division by zero.

RAI 20: Section 5.1.2:

There is a discussion on the impact of convective current aided by hydrogen recombiners on reaching a homogeneous condition inside the containment atmosphere. Please provide the results of typical calculations where gas mixing inside U.S. EPR containment is shown to eliminate stratification, with and without recombiners.

Response 20:

Tests with hydrogen recombiners have shown that exit temperatures can reach 200 – 300 K higher than inlet temperatures. As a consequence, a significant buoyancy-driven flow should

appear in the vicinity of the recombiners. The coarseness of a lumped parameter code like MAAP4.0.7 does not lend itself to fine resolution of the mixing phenomena; however, the sigma criterion for flame acceleration was derived from sparsely instrumented test programs similar to the scale of volumes modeled with MAAP4.0.7. As a consequence, flame acceleration can be adequately predicted. Uncertainties with regard to combustion are addressed by the conservative assumptions applied to hydrogen generation during a severe accident (i.e., 100% clad-water reaction).

RAI 21: Section 5.1.2.1:

It is stated that "in the event that combustion should occur in an equipment room, the effects of detonation could be locally significant, but the containment would be shielded from the internal compartment event and only minimally affected." Please elaborate. It may be true that local detonation may not affect the containment directly, but what about loop piping and potential for indirect failure of the containment as a result of vibrations and piping shakedown?

Response 21:

For the Combustible Gas Control System performance analysis, it is expected that the likelihood of detonation will be eliminated. In the event of hydrogen deflagration, the loads to the environment will be calculated using the adiabatic isochoric complete combustion (AICC) pressure (which is conservative). These loads will then be assessed against the containment ultimate pressure. Presentation of the expected limit AICC pressure vs. containment ultimate pressure will be provided in the DCD.

RAI 22: Section 5.1.2.2:

It is stated that much of the hydrogen from MCC1 is expected to auto-ignite. Please elaborate. What are the conditions inside the cavity? What calculations have been performed to prove this?

Response 22:

Hydrogen auto-ignites in oxygen rich environments at temperatures greater than 1060K. After vessel failure, corium temperature in the reactor cavity and spreading room are well above 1060 K. Both compartments have vents to circulate air from other compartments, allowing for fresh oxygen to be available for combustion. Hydrogen is released from concrete through the ablation process, and travels through the corium to the cooler oxygen rich air. These conditions allow for ignition to occur without an ignition source.

To demonstrate U.S. EPR hydrogen mitigation features under extreme conditions, the uncertainty analysis supporting performance analyses for severe accident response features (to be provided in the DCD) will assume that auto-ignition does not occur (maximizing hydrogen concentration). A supplementary calculation to the Combustible Gas Control System performance analysis will accompany the uncertainty analysis to demonstrate the impact of auto-ignition of hydrogen from MCC1 sources. It is anticipated that the auto-ignition of hydrogen will significantly reduce the total amount of hydrogen in the containment.

RAI 23: Section 5.2.1.2:

It is stated that "global" and "local" types of failure differ significantly in their impact on subsequent accident progression. How exactly do these types of failure affect accident progression, specifically, their impact on core concrete interaction and melt spreading? It is stated further that "subsequent evaluations suggest that this additional margin was associated with water flowing between cracks within solidified debris and gaps that formed between solidified debris and the vessel." Please provide the experimental evidence to prove this hypothesis.

Response 23:

“Global” and “local” failures impact the timing of melt emptying from the vessel and therefore affect the ablation rate, hydrogen generation, heating of containment, etc. The U.S. EPR’s temporary melt retention feature moderates the effect of the different reactor vessel failure modes by confining the melt until most of the core melt has been released from the RPV. The subsequent ex-vessel progression of a severe accident is dependent on the amount and timing of energy imparted. As an example, large releases associated with a global failure will attack the sacrificial concrete quickly, while small initial melt releases from the RPV will result in slower concrete attack. It is therefore the nature of the U.S. EPR retention concept to eliminate the uncertainties associated with reactor vessel failure; thus, corium entering the spreading compartment appears in common physical states regardless of reactor vessel failure mode.

Water ingress into the corium debris significantly changes the heat transfer rate from the debris. Gaps between the debris and the vessel can be expected to form when vessel wall temperatures reach a point where significant creep occurs and molten material is not well adhered to the wall. Allowing for water ingress into the corium debris stabilizes the debris significantly faster than assuming the debris is impermeable. The survival of the TMI-2 reactor pressure vessel has been attributed to the effectiveness of gap cooling.

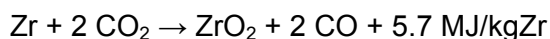
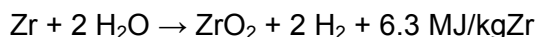
Experimental evidence of these phenomena can be found in Reference 45 cited in the Severe Accident Evaluation topical report. The MAAP4.0.7 analyses performed for the U.S. EPR do not credit water ingress and gap cooling, therefore the model allows for early vessel failure.

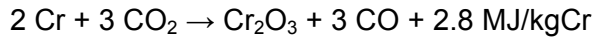
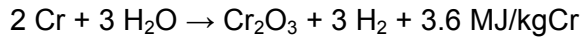
RAI 24: Section 5.2.2:

Please provide the details of chemical reactions that are expected inside the reactor cavity for corium and sacrificial concrete constituents, with the resulting products and their measured thermo-physical properties as applicable to U.S. EPR conditions.

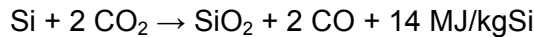
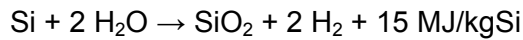
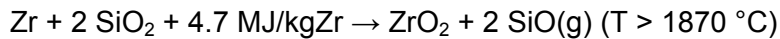
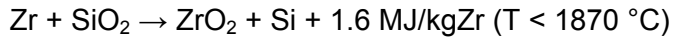
Response 24:

The core melt is continuously heated by the radioactive decay of the fission products in the melt. Another heat source is the chemical reaction heat. The most important chemical reactions in the pool are related to the oxidation of metals by the concrete decomposition gases:





Also the reduction of SiO_2 and Fe_2O_3 by zirconium plays an important role:



Listed below are the most important reactions that take place when concrete is heated. The exact reaction temperatures depend on the heating rate and pressure.

- 100 °C: Loss of evaporable water.
 $\text{H}_2\text{O}(\text{l}) + 2258 \text{ kJ/kgH}_2\text{O} \rightarrow \text{H}_2\text{O}(\text{g})$
- 100–850 °C: Dehydration of hydrates.
 $3 \text{ CaO} \cdot 2\text{SiO}_2 \cdot 3\text{H}_2\text{O} \rightarrow 2\text{CaO} \cdot \text{SiO}_2 + \text{CaO} \cdot \text{SiO}_2 + 3 \text{ H}_2\text{O}(\text{g})$
(Similar reactions for other hydrates; the reaction heats of these endothermic reactions are about 250–500 kJ/kg-hydrate)
- 400–600 °C: Dehydration of calcium hydroxide.
 $\text{Ca}(\text{OH})_2 + 1340 \text{ kJ/kgCa}(\text{OH})_2 \rightarrow \text{CaO} + \text{H}_2\text{O}(\text{g})$
- 574 °C: Crystalline transformation from α - to β -quartz.
 $\text{SiO}_2(\alpha) + 12 \text{ kJ/kgSiO}_2 \rightarrow \text{SiO}_2(\beta)$
- 600–900 °C: Decomposition of calcium carbonate.
 $\text{CaCO}_3 + 1637 \text{ kJ/kgCaCO}_3 \rightarrow \text{CaO} + \text{CO}_2(\text{g})$
- 1200–1500 °C: Melting of Portland cement.
- 1423 ± 50 °C: Melting of quartz.
 $\text{SiO}_2(\text{s}) + 130 \text{ kJ/kgSiO}_2 \rightarrow \text{SiO}_2(\text{l})$
- 1462 °C: Decomposition of hematite into magnetite.
 $6 \text{ Fe}_2\text{O}_3 + 480 \text{ kJ/kgFe}_2\text{O}_3 \rightarrow 4 \text{ Fe}_3\text{O}_4 + \text{O}_2(\text{g})$
- 1597 °C: Melting of magnetite (Chase, 1998)
 $\text{Fe}_3\text{O}_4(\text{s}) + 600 \text{ kJ/kgFe}_3\text{O}_4 \rightarrow \text{Fe}_3\text{O}_4(\text{l})$

In addition, CaO and SiO_2 may form some compounds, like CaSiO_3 , but the phase diagram of these is very complex.

From the reactions, it can be seen that water vapor and carbon dioxide are released from concrete when it is heated from 100 to 900 °C. Siliceous concrete releases mainly water vapor, while calcareous concrete releases also substantial amounts of carbon dioxide.

RAI 25: Section 5.2.2.2.2:

Please provide the basis for the following assertions: (1) "This situation [melt stratification with metallic melt below oxide] will only occur shortly before gate failure at a time when all corium is already added to the MCCI pool.", and (2) "In the mixed mode the ablation rates are generally lower, so the protective layer will be reached by the melt much later and at about the same time as the melt reaches the gate."

Response 25:

The prediction that layer inversion between the initially heavier core-oxides and the lighter metal/slag on top always occurs before the melt reaches the gate is a conclusion drawn from experimental programs like CORESA and complemented by plant-specific analyses performed for the OL-3 project in Finland. The analyses, which involved several conservative assumptions for the demonstration of the accumulation function (i.e., early predicted contact between melt and gate), consistently demonstrated layer inversion before gate failure. The principal conservatisms are (i) the assumption of equal axial and radial heat transfer coefficient from the molten pool, and (ii) the neglect of the mass of the concrete bumpers in the lower pit. These assumptions have been carried over to analyses performed with MAAP4.0.7.

Nonetheless, the validation of the melt stabilization system function does not rely on the preceding layer inversion in the pit. Based on tests with oxide melts, successful gate opening and melt spreading are also expected under the assumption of a layered configuration with the dense core-oxides still at the bottom.

RAI 26: Section 5.2.3:

*What is the degree of penetration of the protective layer before the melt gate is contacted?
What are the uncertainties?*

Response 26:

The possibility of penetration into the protective layer is not excluded in the U.S. EPR design; however, ablation rates into this layer are significantly less than those associated with the sacrificial concrete. The major uncertainties are related to the ratio of radial-to-axial ablation rates. The inclusion of the protective layer addresses these uncertainties. The protective layer in the U.S. EPR will consist of sintered zirconia bricks about 20 cm thick; these bricks have been shown in experiments to halt the ablation process. Zirconia is fully stable against metal melts in the expected temperature range and the oxidic corium melt will be kept in a temperature range by MCCI that avoids a destructive interaction. In Section 5.2.3.5 of the topical report, the ablation rate of zirconia by a superheated oxidic corium (following MCCI) was identified to be less than 2 cm/hr. In section 5.2.3.9 of the topical report, the ablation of the sacrificial concrete, which is 50 cm thick, is expected to take about 2 hours before the gate is reached. Therefore in the unlikely event that the metal layer of corium quickly ablates the sacrificial concrete to the protective zirconia and the layers then flip so that the oxidic layer is in contact with the zirconia, only about 20% of the zirconia block would ablate (4 cm of 20 cm). This is a very conservative estimate because in this situation concurrent MCCI is expected to

reduce the erosion rates on the protective concrete.

Melt retention analysis has shown that sacrificial concrete will be incorporated into the melt prior to melt gate contact. This behavior along with the protective layer predefines the maximum and most probable amount of sacrificial concrete that can be added during melt retention in the pit. As a consequence, the retention function becomes independent of the uncertainties regarding 2D-melt progression.

RAI 27: Section 5.2.4.4:

It is stated that during MCCI, as a result of melt stratification (metal at bottom with light oxide on top), the water that pours onto the melt will contact the oxidic melt fraction and the sacrificial concrete layer mainly interacts primarily with the metallic melt. What are the consequences of a mixed layer, i.e., a heterogeneous mixture of metals and light oxides as a result of mixing and gas sparging? It appeared in the OECD-MCCI tests, that the water ingress was dependent on the material and that the addition of concrete to the melt reduced the water ingress. How do these experimental findings affect the top cooling of the "conditioned" melt (i.e., core debris mixed with sacrificial concrete in the cavity) in the spreading subcompartment?

Response 27:

A consequence of the expected stratification of the melt during and after MCCI is that the water, which pours onto the surface of the melt, will come into contact with the oxidic melt fraction. The flooding and quenching of oxidic melts, including prototypic corium, have been extensively studied in the framework of the MACE and OECD-MCCI programs. The obtained results unambiguously demonstrate that water will spread on the molten surface smoothly, without any energetic interaction. Further, these tests indicate substantial superficial fragmentation and improved coolability at the surface, promoted by the ongoing interaction between the water and the concrete and the mixing provided by released gas. The fast formation of an oxidic crust limits the contact time between melt and water.

At the time flooding starts, the melt is subject to an intense convective mixing, driven by concrete decomposition gases. This causes a steady introduction of hot material to the surface and a high convective heat flux at the interface with the water. As a result, the surface temperature remains high so that film boiling can stay the dominant heat transfer mode.

In the film boiling regime, efficient heat transfer is anticipated owing to conduction and radiation across the agitated (i.e. area enhanced) melt-water interface. In addition, melt droplets will be entrained into the water overlayer by sparging gas. The resulting early heat fluxes, as measured in the MACE program, are in the range of $>2 \text{ MW/m}^2$.

With cool-down proceeding, the melt will then enter a transient bulk-freezing phase. Since solid oxidic corium has a higher density than the liquid, fragments of frozen material (formed at the surface) will be re-mixed into the molten pool and will cause an overall decline in temperature. This process leads to a collapse of the gas film and eventually to the formation of a slurry-type, viscous oxidic melt. The drop in surface temperature, which results from the switch to gas-enhanced nucleate boiling, is accompanied by the formation of a surface crust.

The late bulk-freezing phase is characterized by a strong decline in superficial heat flux to almost zero. In this state the melt becomes thermally "insulated" from the water. As a consequence, bulk temperature starts to rise again (due to decay heating) and convection is re-

established. The temperature of the melt and the thickness of the crust then approach steady-state – governed by the level of internal decay heat generation.

The forming crust can provide support for melt particles and droplets that drain through cracks and holes into the water with the flow of concrete decomposition gas. Such melt ejections through volcano-like structures have been observed in experiments with simulant and prototypic material. The created particle bed transfers its internal decay heat directly to the water. Effective cooling is also achieved within porous regions of the crust potentially created by thermal cracking.

The MAAP4.0.7 code does not currently have the inherent models necessary to capture these phenomena. It does provide a means to approximate this behavior using user-defined functions. A user-defined function has been implemented to emulate the three distinct heat transfer phases. The first phase is the period in which molten corium is in contact with water. With early high heat fluxes, there is enough energy to vaporize all incoming coolant (< 100 kg/s). The duration of the flooding period depends primarily on what fraction of the energy initially stored in the melt can be released to the water. A best-estimate value of that interval is between 1000 – 2000 s.

After the end of the initial flooding period, the rate of steam generation becomes less than the flooding rate, so water starts to accumulate atop the melt. The melt state at that time can be assumed to consist of some fragmented oxide layer atop a bulk at a relatively low temperature. The decay power released within the fragmented part is transferred directly to the water, while the decay power in the bulk will first be used to re-heat the melt. For low fragmentation levels, this power is not sufficient to raise the temperature of the incoming water to the saturation level; hence, the steaming rate is assumed to be zero. During this period, it can be assumed that all the decay heat goes into reheating the melt. A prolonged degraded heat transfer period will elevate the melt temperature, increasing the sensible heat of the corium pool. This will result in a longer period for melt stabilization and, hence, a long period of steaming to the containment once nucleate boiling heat transfer is established. Depending on the fragmentation and decay heat level, a best-estimate for this duration of this period is between 5000 – 7000 s.

Following this period, the pool is expected to be saturated and steaming will commence. The steam rate is driven by decay heat. For a high decay heat level, characteristic of a rapidly progressing severe accident, the steam rate has been estimated to be about 11 kg/s.

Considering the large uncertainties associated with this process, heat transfer from the spreading compartment is explicitly treated in the uncertainty analysis being prepared for the DCD. Since WALTER, rather than MAAP4.0.7, is being applied to characterize core melt stabilization, uncertainties considered in the MAAP4 input are biased to conservatively address the impact of steaming on containment pressure.

RAI 28: Section 5.2.4.5:

What is the stability boundary of two-phase water flow through the melt stabilization channels for U.S. EPR under the expected range of heat flux and temperature conditions? Please elaborate on the BENSON test rig and the CHF (Critical Heat Flux) conditions in the cooling channels.

Response 28:**Test facility and experimental matrix**

[

]

Two water supply modes were investigated: co-current and counter-current flow. The first simulates the situation in which the water within the channel flows in the same direction as the steam. This is the normal case, e.g. during the initial fill-up of the spreading area and during active cooling. Co-current conditions do also exist, at least on average, during the entire period of passive operation, because there is a steady flow of water through the channels to compensate the water evaporated at the upper surface of the melt.

True counter-current flow conditions only occur if, temporarily, there is no inflow from the IRWST or in cases when the SAHRS terminates active mode of operation. When the SAHRS pumps are turned off, water from the pool atop the melt could flow backwards into the sump through the cooling channels.

In addition, counter-current flow conditions could occur during passive operation, as evaporated water is replaced, thus inducing a very small flow velocity. Local reverse flow conditions may thus sporadically occur within individual channels, or within groups of them. In this sense the passive cooling mode does not explicitly require co-current conditions in all of the parallel channels.

About 15 tests with counter-current (self-regulating) and co-current (enforced water supply rates of 0.1 kg/s and 0.2 kg/s) flow conditions were performed. The values of imposed heat flux and channel inclination were varied between 20-120 kW/m² and 0°-2°, respectively. The tests were conservatively performed at 1 bar; however, realistic containment pressure for such an event will likely be > 2 -3 bar, which would almost double the heat flux extractable in the cooling channels – significantly increasing the margins inferred from these tests.

Obtained results

The experiments showed that up to a level of 40-80 kW/m² (dependent on inflow condition and inclination) the heat transfer to the water does not lead to stratified flow conditions in the channel. Instead, the top of the channel remained wetted and effectively cooled by the water. This led to generally low temperatures of the cooling structure. Measured values even near the heater position (TCs at -1 cm) were only 50 – 80 K higher than the water temperature.

At higher heat fluxes, departure from nucleate boiling (DNB) and resulting stratification of the 2-phase flow were observed. Two different variants of DNB occurred, depending on the heat flux and the mode of water inflow, characterized by either:

- a temperature profile with a distinct maximum at a certain position of the flow channel, usually at about a flow length of 2 – 3 m (from the entrance). In front of this location and also further along the channel, temperatures remained low; or
- high temperatures along the entire channel (except in co-current mode, close to the entrance of the water)

Due to the thickness of the channel walls and the corresponding thermal resistance and heat capacity, the evolution of steady-state temperatures took several hours for both variants of DNB. The rate of temperature increase was typically in the range of 1 K/min.

Analysis with the WALTER code suggested that the imposed heat flux from the top of the channel could be associated with certain temperature profiles within the cooling structure and with the wetting ratio in the water flow channel. Accordingly, even for the highest investigated heat flux from the top, 120 kW/m², the related minimum water level was only about 4.5 cm (45% of the channel height of 10 cm). This heat flux is about twice the expected maximum steady-state heat flux from the melt.

Considering the benign behavior of the heat transfer at 120 kW/m², it was concluded that the given channel geometry could tolerate even higher heat fluxes. The performance of such tests was, however, prevented by the fact that for higher heat fluxes, the temperature at the top of the channel would have exceeded the burn-out limit of the heating elements of about 650°C.

Conclusions on heat transfer

The heat transfer from the sideward cooling structure to the water in the vertical channels does not constitute a problem, as the margins to the related CHF limits of > 1 MW/m² are high. Moreover, the experimental results demonstrate that there is also sufficient margin for the heat transfer to the water in the horizontal cooling channels at the bottom.

The effective operation of the channel under counter-current flow conditions is taken as a proof that heat transfer is not sensitive to the water inflow conditions. This eliminates problems with respect to a potentially non-uniform water supply to the individual channels. Cooling is thus highly reliable, if the channels are kept submerged. Even without operating the SAHRS, this is achieved by the connection and passive inflow of water from the IRWST. Due to the effective cooling, complete solidification of the metallic and oxidic melt fractions will typically be achieved within a few hours or days, respectively. The predicted solidification times depend on the assumptions regarding (i) the degree of superficial fragmentation and (ii) the spatial distribution of the metallic and oxidic melt phases.

RAI 29: Section 5.2.5:

Melt retention in the cavity is necessary for successful ex-vessel cooling and melt spreading. Is it considered conceivable that the concrete above the melt plug could crack or fragment in contact with core debris, thus cutting short the amount of ablation required to reach the melt plug and premature failure of the plug? What analysis has been done to prove that practically the entire core inventory will be collected in the cavity prior to spreading and stabilization? What is the effect of jet impingement on the substrate in the cavity pit under both metallic and oxidic melts?

Response 29:

Spallation-type failure of concrete can occur in vertical concrete walls when they are exposed to high temperatures for sufficiently long times, e.g. in case of fires. Due to their vertical orientation the outer concrete layer is not mechanically stable and can detach from the wall as a result of thermal and dead-weight stresses and fast evaporation of the physically bound water.

With MCCI, the fluid pressure within the melt, in combination with the melt's high local viscosity and surface tension, safely prevents the fragments from detaching from the surface. As a consequence, the concrete decomposition products melt and form a glassy phase at the interface, especially if the concrete is of siliceous type, which is the case for the sacrificial concrete of the U.S. EPR. This behavior is consistently confirmed by the results and observations from the set of available MCCI experiments.

The KAJET experiments performed at Forschungszentrum Karlsruhe (FZK) showed that significant concrete erosion will only occur if melt jets are stable and well-focused and if they have a long duration and high velocity. Additional experiments examining melt poured onto a concrete surface have shown only limited erosion. This is attributed to the fact that the decomposition of concrete creates a large amount of gas, which counteracts and disperses the impact of the melt. The possible extent of concrete erosion in the lower pit is further limited by the fact that the earlier released melt will accumulate at the lowest level and thus protect the melt plug.

To focus such a jet, a small hole would have to form and be sustained. Small holes in the RPV are only considered possible for vessels with preexisting penetrations in the bottom. The lower head of U.S. EPR RPV has been designed without preexisting penetrations. If the RPV failure is to be caused by the preceding heat-up by the molten pool, the ultimate failure region would be too large to result in a focused jet, and the resulting release period would be correspondingly short. In addition, the expected failure position would be near the surface of the molten pool, where heat fluxes are much higher than at the bottom.

As a consequence, the risk of jet impact on the U.S. EPR melt plug, which is the key element that should not fail prematurely, is considered negligibly low, in particular as jets require high internal pressure which is prevented by early depressurization of the primary circuit.

Along the circumference of the vessel, local melt discharges could potentially occur and hit the adjacent cylindrical concrete walls around the pit. For such local discharges, temporary impact would not impede the retention function of the pit because the sacrificial concrete is backed-up by a cylindrical protective layer. Sufficient stability of the zirconia-based material against metallic and oxidic corium melts has been experimentally demonstrated as described in the topical report.

As part of the analyses being prepared for the DCD, the retention and condition function of the reactor cavity will be demonstrated within the context of the uncertainty analysis methodology described in the RAI 14 response.

RAI 30: Section 5.2.5:

It is possible that some core material could relocate from the reactor vessel at a time following failure of the reactor cavity melt plug. What implications would such late-failing debris have on discharge to and cooling or MCCI inside of the spreading chamber?

Response 30:

This scenario is considered to be reliably excluded for the U.S. EPR design. Such an outcome is significantly limited by the retention phase, which maximizes the core melt release prior to failure. A bounding scenario which could result in late releases would involve a late active reflood of the RPV. Considering that the preceding outflow of all molten pools would, as a consequence, result in only small, shallow melt pools remaining, late releases would be negligible as it would be likely that the late addition of water would quench, cool, and stabilize the material still inside the residual RPV.

RAI 31: Section 5.4.1.2:

It is stated that "In traditional severe accident space, single failure is not a consideration in system design; however, the U.S. EPR severe accident systems can accommodate such a failure and still perform their function," Please elaborate if this is true for all severe accident mitigation systems in U.S. EPR.

Response 31:

The context of this statement, as given in Section 5.4.1.2 of the topical report, referred to the CGCS (PARs) and SAHRS performance. Since the release of the topical report, AREVA has chosen to rely on a single SAHRS train. Given the long lead time prior to SAHRS actuations, AREVA considers the reliability of the SAHRS sufficient with a single train. As such, the topical report will be updated to reflect this design change. With regard to other severe accident response features, primary system depressurization and the initiation of passive flooding to the spreading compartment are also considered to be tolerant of a single failure through use of two severe accident valve trains (see Section 2.2.1 in the topical) and two initiators/passive flooding valves (see RAI 9 response), respectively.

RAI 32: Section 6.1:

Please provide more details on the flow of data among the MAAP4, MELTSPREAD, and WALTER codes that is sketched out in Figure 6-1 of the topical report. Specifically, what MAAP4 input parameters are impacted by the results of the MELTSPREAD and WALTER calculations?

Response 32:

MAAP4.0.7 has been developed to address key phenomena associated with the U.S. EPR's severe accident response features. Given the long time domain necessary for severe accident simulations, some phenomenological modeling simplifications are necessary to facilitate reasonable calculation execution. Modeling of melt spreading and stabilization dynamics are among those simplifications. MELTSPREAD and WALTER are separate-effects analysis codes for investigating melt spreading and stabilization, respectively. Analyses performed by these codes utilize outputs from MAAP4.0.7 simulations. In particular, these codes apply MAAP4.0.7 results for melt conditions, i.e., mass, temperature, and composition, as input. Code results

from MELTSPREAD and WALTER are not used in MAAP4.0.7 analyses; although, in some circumstances, code results are used to reinforce modeling assumptions (e.g., rapidity of the spreading process). Figure 6-1 will be revised to remove the link leading from the WALTER code to MAAP4.0.7.

RAI 33: Section 6.1.1:

Please provide subroutine descriptions for all new models added to MAAP to analyze the U.S. EPR design. Describe the status of peer review for MAAP4.07 models as part of the present U.S. EPR submission process). Also discuss any MAAP4 model validation for the new core barrel, melt relocation, and the impact of the heavy reflector.

Response 33:

The NRC has obtained the beta version of MAAP4.0.7 and therefore has access to the latest subroutine descriptions.

The MAAP4.0.7 code has been under development and testing by FAI and AREVA NP since Fall of 2005. During early 2007, the MAAP4.0.6 code was updated with the code modifications sponsored by AREVA NP along with code improvements sponsored by the MAAP Users Group to create the first version of MAAP4.0.7. This first version of MAAP4.0.7 has been tested by both FAI and AREVA NP and passed the FAI QA process. MAAP4.0.7 is now under review by EPRI in preparation for its planned release later in 2007.

The validation of the core barrel/heavy reflector model is described in subroutines CBLFAIL, MOVECR and HEATUP.

RAI 34: Section 6.1.1:

Has the second order Runge-Kutta integration method been used for this analysis? If so, what are the major differences between these results and those obtained using the first-order Euler method?

Response 34:

The MAAP4.0.7 parameter IRUNG provides a user-defined option for specifying the integration scheme used. Calculations performed by AREVA apply the first-order Euler method. This choice is recommended by FAI based on observed numerical problems inherent in the current implementation of the Runge-Kutta scheme.

RAI 35: Section 6.1.1.7:

Is oxidation of the molten steel between the crust and the solid part of the core barrel calculated? If so, how much additional hydrogen is produced?

Response 35:

MAAP4.0.7 calculates the oxidation of molten steel in subroutine SSRACT. This subroutine is called from subroutine PRISYS in order to calculate the stainless steel oxidation in the primary system heat sinks such as the core barrel, vessel wall, upper plenum internals, and the metal layer on the top of the corium bed in the RPV lower head. First MAAP4.0.7 calculates the steam diffusion process in the gas phase. MAAP4.0.7 then selects an appropriate correlation for oxide layer front movement depending on the steel temperature. Based on these calculations, and the availability of steam and steel, the reaction rate is determined on the basis of steam consumption, hydrogen generation, oxygen uptake in steel, and energy generation. More detail is available in the subroutine description for SSRACT. See RAI 19 response for the approximate amount of hydrogen produced from molten steel in the RPV.

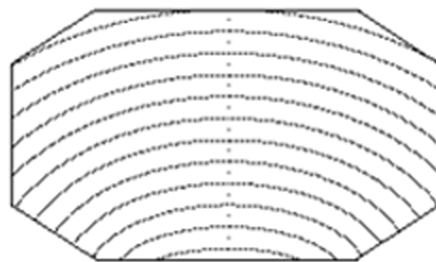
RAI 36: Section 6.1.2:

Please discuss the applicability of 1D MELTSPREAD code to the spreading compartment that is clearly 2D? Were other codes (e.g., THEMA) considered?

Response 36:

Use of MELTSPREAD for the U.S. EPR is confined to the assessment of melt spreading. Normally, the MELTSPREAD code is used with the nodalization model representing the Mk I BWR that has cells moving radially out from the melt discharge channel and a final cell representing the annular portion of the spreading area. The U.S. EPR MELTSPREAD model employs user-specified nodalization to more accurately describe the U.S. EPR CMSS spreading area. A graphical representation of the nodalization scheme is shown below in Figure RAI-36-1. Based on spreading tests, corium is expected to rapidly spread and distribute throughout the spreading area (within minutes of gate failure). MELTSPREAD analyses being prepared for the DCD show that the melt conditioned in reactor cavity performs in this manner. A main objective for MELTSPREAD is to support the MAAP4 simplification that assumes instantaneous relocation from the reactor cavity to the reactor pit.

Figure RAI-36-1 U.S. EPR CMSS Spreading Area MELTSPREAD User-Specified Nodalization



RAI 37: Section 6.2.1.12:

What criteria do users need to use to select the Kutateladze Number for the containment heat sinks? What are the ranges of uncertainty for any model parameters varied?

Response 37:

This feature is new in MAAP4.0.7 and was added to the code so that it would be possible to model the presence of a stable vapor barrier (departure from nucleate boiling) within the cooling channels of the U.S. EPR core catcher. In order to do this, the parameter FCHFHS is set for the spreading room floor and side walls. [

] This value has been found to be sufficiently high so as to not limit the heat flux from the spreading area to the cooling channels, thus allowing the formation of two-phase conditions in the cooling channels.

Melt flooding is the principal heat transfer mechanism for which the Kutateladze model is applied for U.S. EPR severe accident analyses. As stated in Section 6.1.2.12 of the topical report, MAAP4.0.7 provides the capability to assign a user-specified Kutateladze number to model unique heat transfer phenomena. Modeling of the heat transfer phases described in the RAI 27 response is made possible through the use of this MAAP4.0.7 capability. Uncertainty associated with this model is explicitly addressed in analyses being prepared for the DCD. The key parameters are identified in the response to RAI 14, Table RAI-14-2.

RAI 38: Section 6.3:

When will the validation work with MAAP 4.0.7 and MELCOR 1.8.6 be completed? Will the results be presented after design certification begins?

Response 38:

AREVA NP has studied the performance of MELCOR 1.8.6 by analyzing various aspects of the in-vessel melt progression, core melt retention phase in the reactor pit and spreading/stabilization in the spreading room. While some preliminary comparisons between MELCOR 1.8.6 and MAAP4.0.7 have been made, the consistency between the two codes is not at a sufficient level of agreement to permit an in-depth code-to-code comparison. Given the modeling limitations, AREVA NP is no longer pursuing model development and analysis with MELCOR 1.8.6.

RAI 39: Section 6.3.1.1:

The comparison of MAAP with CC2 test (limestone/concrete sand basemat) is satisfactory, while the MAAP ablation predictions of CC3 test (siliceous basemat) showed discrepancies between factors of 2-3. The reason for the differences between the predictions for the two tests is not explained in the topical report. This could impact the MAAP predictions for EPR severe accident calculations. Please explain.

Response 39:

The validation of MAAP4.0.7's ability to predict MCCI phenomena is based on the suite of benchmarks that include several ACE, BETA, SURC, and CCI tests. Given the phenomena are subject to broad uncertainties associated with melt state, melt composition and material properties, ablation predictions within a factor of 2 are reasonable. While many tests have demonstrated a quasi-isotropic heat flux distribution resulting in comparable erosion rates in all directions, CCI-3 showed a rather large discrepancy between axial and radial ablation rates. This discrepancy is not entirely understood; however, for the U.S. EPR this uncertainty has no negative consequences given the protective layer that lines the reactor cavity that will focus energy axially when the ablation front can no longer move laterally. As such, the key comparison between MAAP4 and the experiment is focused on the axial ablation rate, which is within a factor of 2 of the data.

In the U.S. EPR, the largest uncertainty impacting ablation rates is associated with the melt release modes from the reactor vessel. This is largely dependent on assumptions considered for in-vessel progression. Several parameters are considered that will impact melt state, reactor vessel failure, and melt relocation to the reactor cavity (see RAI 14 response). The discussion on core melt stabilization that will appear in the U.S. EPR DCD will highlight the impact of these uncertainties on the eventual failure of the gate supporting the melt plug between the reactor cavity and the spreading compartment.

The CCI-2 and CCI-3 benchmarks were performed using an early developmental version of MAAP4.0.7.

RAI 40: Section 6.3.1.1.3, Figure 6-14:

It is not clear which curve represents the MAAP 4.0.7 results. There are several red curves shown. Please provide a more clear delineation of the various curves.

Response 40:

Following are two graphs which delineate the data in Figure 6-14 between the basemat and the sidewall:

Figure RAI-40-1 MAAP4.0.7 Predicted Average Melt Temperature vs. CCI-2 Data (Basemat Only)

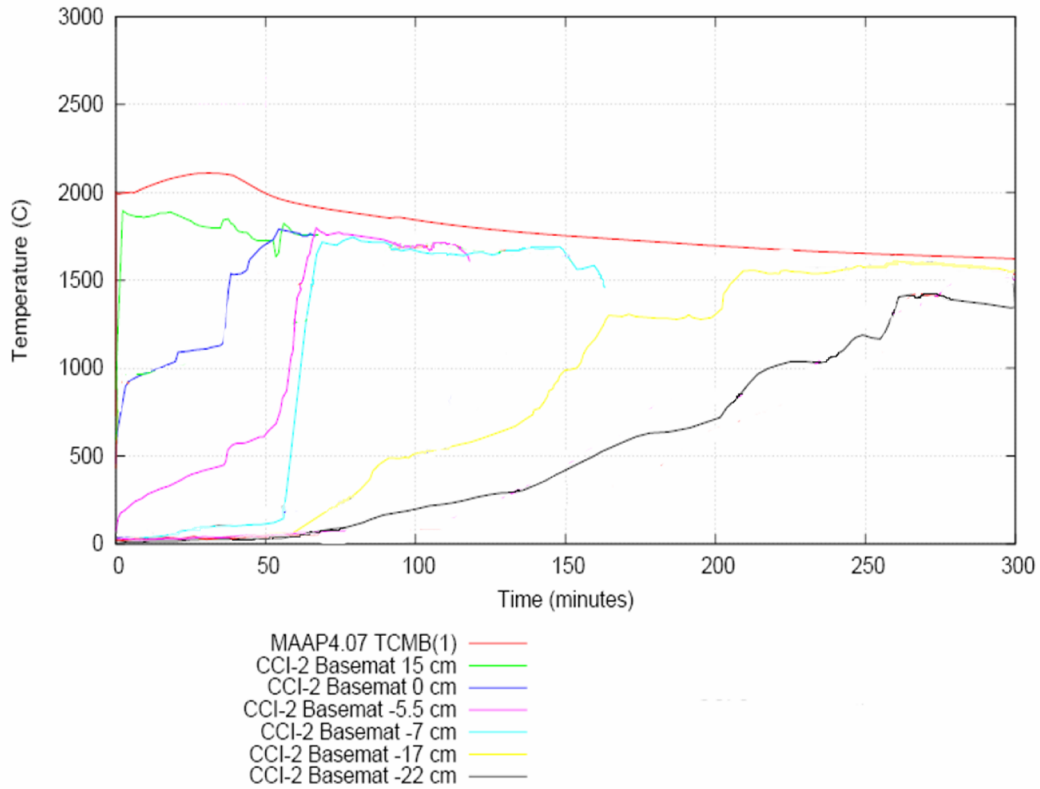
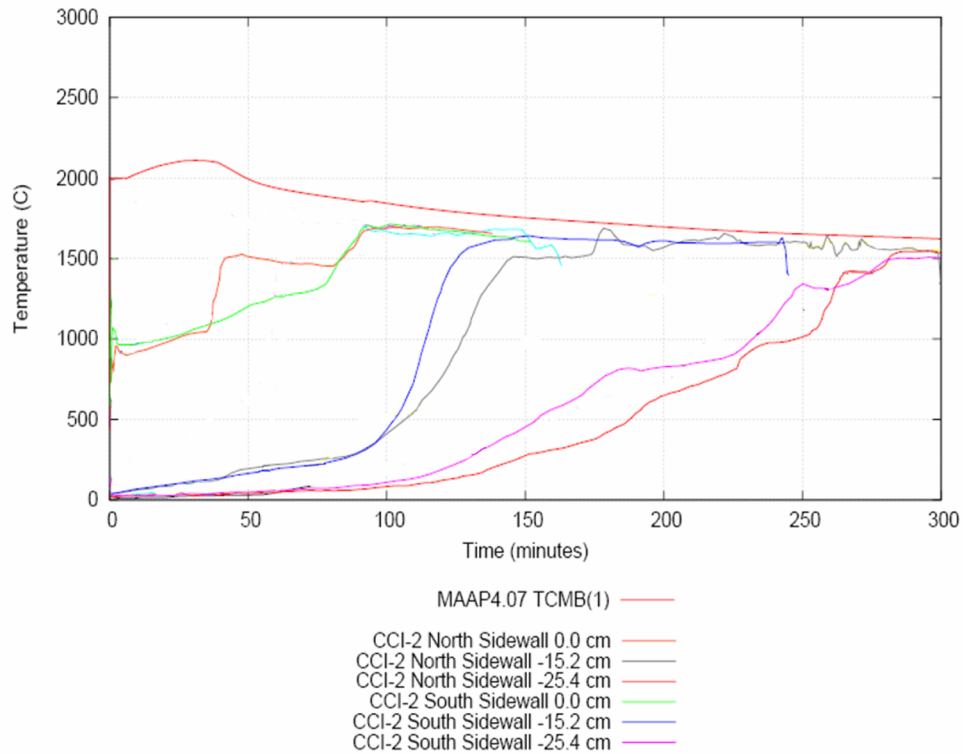


Figure RAI-40-2 MAAP4.0.7 Predicted Average Melt Temperature vs. CCI-2 Data (Sidewall Only)



RAI 41: Section 6.5.1, Table 6-9:

What is the reason for not including (in Table 6-9) induced SGTR (Steam Generator Tube Rupture) scenarios that may be relevant under the "RCS [Reactor Coolant System] Depressurization" issue?

Response 41:

Table 6-9 in the topical report presents "Possible Representative and Bounding Scenarios identified to address key severe accident issues" to be included in the calculation matrix developed to address severe accident safety issues. The scenarios identified in Table 6-9 are those considered "probable candidates". Relevant scenarios are defined as those having a Core Damage Frequency (CDF) greater than $10^{-8}/\text{yr}$. Analysis of these cases establishes a baseline performance measure for the design. The verification goal for this scenario class is to show that the severe accident response features function as designed and that the operability of the containment system is maintained. Large uncertainties exist as to what initiating events and coincident occurrences lead to a severe accident. The final suite of event scenarios addressed for U.S. EPR design certification will be based in terms of the most probable initiating events and the likely Core Damage End States (CDES). The list of "Relevant Scenarios" given in Table

6-9 of the topical report considered preliminary PRA Level 1 and 2 results which reported a CDF below 10^{-8} for the SGTR scenario. Therefore, the SGTR scenario is not considered “relevant”.

RAI 42: Section 6.5.1:

It is recognized that simultaneous release of corium and water from the RPV is one of the bounding scenarios that will be considered (Table 6-9). How would the presence of any water inside the cavity and melt discharge channel (e.g., from injection sources to the failed RPV) affect the melt discharge from the cavity, and its subsequent relocation into the spreading compartment?

Response 42:

The uncertainty analysis, as mentioned in Section 6.5.2, accounts for a broad spectrum of uncertainties that exist in severe accidents. In evaluating the inputs for the uncertainty analysis, the amount of accumulator injection was considered as a biased parameter such that the number of accumulators providing water to the reactor vessel resulted in the most penalizing condition with regard to hydrogen generation and corium temperatures. While accumulator injection is not considered a “late” safety injection situation, in many instances, accumulator injection will follow core damage. Beyond the most penalizing condition, further addition of water was found to lower temperatures and, as a consequence, reduce hydrogen generation and hasten core melt stabilization. For the flow rates typical of safety injection – which are similar to that expected from passive flooding of the spreading compartment – and the relatively small contact area in the reactor cavity, it is not reasonable to expect that safety injection appearing in the reactor cavity would have a significant impact on melt stabilization prior to gate failure. As such, corium temperatures in the reactor vessel and melt conditions are not expected to be significantly altered by the presence of safety injection coolant. Corium is expected to relocate smoothly out of the reactor cavity, through the discharge channel and into the spreading compartment following gate failure.

Gate blockage, possibly resulting from solidified corium or some detached RPV component, is considered in the uncertainty analysis. The “best-estimate” expectation is that 100% of the gate will fail. This may occur as a local failure followed by complete gate failure as the flow of corium into the spreading room melts away any remaining solid material. Nonetheless, to address this uncertainty the gate was sized such that even with significant blockage (see RAI 14 response), complete melt relocation from the reactor cavity to the spreading compartment would occur rapidly.

RAI 43: Section 6.5.2:

Please address uncertainties in determining the recombination rate in the recombiners.

Response 43:

[

]

The uncertainty associated with PAR performance is explicitly treated in the uncertainty analysis being prepared for the DCD.

RAI 44: Section 7.0:

From among the scenarios selected for a bounding analysis of accidents with MAAP4, why was no scenario chosen involving high reactor vessel pressure up until the moment of vessel breach? Would high pressure alter substantially any of the findings with respect to parameters such as time to vessel failure, quantity of hydrogen generated, etc.

Response 44:

The scenarios shown in Section 7 (LBLOCA, LOOP, and SBLOCA) are general in nature and were originally presented as sample problem scenarios. A scenario with high Reactor Coolant System (RCS) pressure at time of Reactor Vessel (RV) failure had not yet been developed at the time of the topical report submittal.

Scenarios to be explicitly addressed for the purpose of safety issue resolution and documented in the DCD are those defined as “relevant” scenarios. The method for choosing which scenarios are relevant is mentioned in Section 6.5.1 of the topical report. Relevant scenarios are defined as those having a Core Damage Frequency (CDF) greater than 10^{-8} occurrences/year. Based on the results of the PRA Level 1 analysis, these relevant scenarios include: three Loss of Offsite Power (LOOP) scenarios (each reflecting a different core damage end state), one Small Break Loss-Of-Coolant-Accident (SBLOCA) scenarios and Loss of Balance of Plant (LBOP) scenario. In the uncertainty analysis being prepared for the DCD, the most probable RCS pressure at the time of RPV failure is expected to be approximately that of the containment (~2 – 3 bar). This is a consequence of the credited manual actuation of the severe accident depressurization valves. Uncertainty with regard to the timing of this manual action is examined in the uncertainty analysis, thus raising the possibility of higher RCS pressure at the time of RPV failure. The peak RCS pressure at the time of RPV failure will serve primarily as input to a discussion on the U.S. EPR’s tolerance to High Pressure Melt Ejection and subsequent Direct Containment Heating. Given the statement in Section 2.2.3.1 of the topical report that reactor cavity structures will be tolerant to structural forces equivalent to 20 bar, 20 bar will be used in several analyses to support that objective. The uncertainty analysis is expect to validate that 20 bar bounds the domain of relevant scenarios.

For those events in which RCS pressure at the time of RPV is shown to be above the containment pressure (and < 20 bar), phenomenological differences in event progressions as a function of this measure are not expected to be significant. For example, several factors enhancing hydrogen generation (i.e., presence of steam, rate of metal-water reaction, structural integrity of core) are dominant at the time of core damage when RCS pressure is high for many

events. One possibility is that the high pressure could contribute to a creep rupture failure at a location other than the RPV. This is being investigated in analyses being prepared for the DCD.

RAI 45: Section 7.0:

A SBLOCA scenario with EFW (Emergency Feed Water) was selected as the limiting case with respect to hydrogen production. Would the limiting case not be better represented by a scenario involving some recovery of injection capability after the start of core degradation, so as to maximize the amount of steam available?

Response 45:

The scenarios shown in Section 7 (LBLOCA, LOOP, and SBLOCA) are general in nature and were originally presented as sample problem scenarios. Analyses prepared for the U.S. EPR design certification consider several phenomenological and process uncertainties to identify the limiting conditions that challenge the U.S. EPR's severe accident response features (see RAI 14 response for more detail). At high temperatures, the addition of water can either increase hydrogen generation by providing more "fuel" for reaction with cladding and stainless steel or decrease hydrogen generation by enhancing heat transfer from the fuel rod. The uncertainty analysis being prepared for the DCD will explicitly consider late accumulator safety injection as a consequence of RCS depressurization following the signal indicating core damage (core exit temperature greater than 650 °C, 1200 °F). Spurious or operator actuated safety injection not initiated by an automatic function will not be examined in the analyses prepared for the U.S. EPR DCD.

RAI 46: Section 7.3.1:

Please provide more information on the LBLOCA scenario, namely:

- a) *The initiator for the LBLOCA scenario was taken to be a severance of the pressurizer surge line. Since the rationale for this scenario was as a bounding case with respect to melt stabilization and early containment pressurization, why was a larger break not analyzed?*
- b) *Following lower plenum dryout at 2 hours (Figure 7-8), there is still about 20 tons of water in the RCS. Where is this water coming from?*
- c) *Is the fraction of the core/reflector in the lower plenum at the time vessel breach (see also Figure 7-11 and 7-12) a conservative estimate for melt spreading and stabilization.*
- d) *The MAAP analysis shows extremely efficient melt quenching evidenced by the corium temperature (Figure 7-25), and rapid containment pressurization (Figure 7-14) in about one hour. What is the modeling assumption in MAAP? Is the bottom cooling modeled?*
- e) *In the period between about 10 and 20 hours, total containment pressure (Figure 7-14) is about 2.5 to 3.5 bar, and the average air mole fraction (Figure 7-16) is about 0.15 to 0.20, implying that the average partial pressure of air is only about 0.5 bar. Since no*

failure of containment was mentioned in the calculation results, where has the rest of the air gone (approximately 1.0 bar at the beginning of the scenario?)

- f) *How much time is required for the melt in the reactor cavity to reach the stabilized melt conditions that are desired prior to melt transfer? Does an adequate margin of time exist within which to guarantee these melt conditions?*

Response 46:

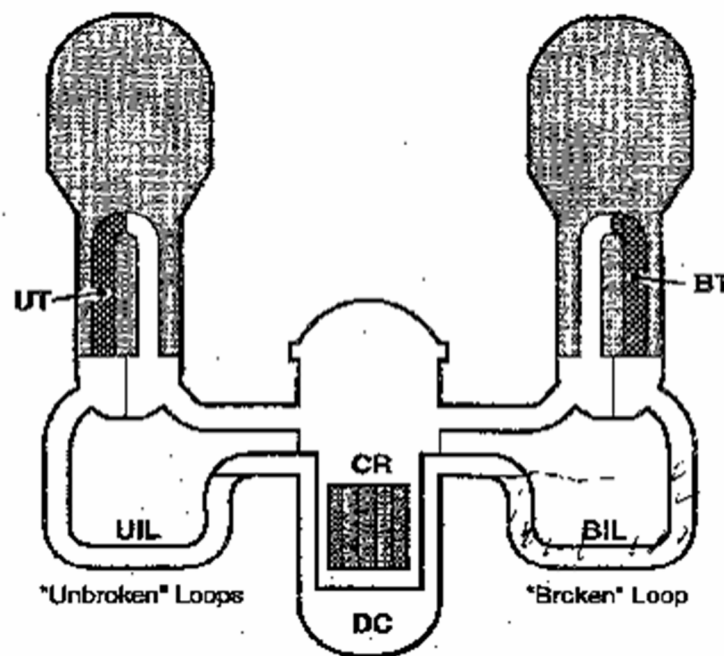
- a) The initiator for the LBLOCA scenario was taken to be a severance of the pressurizer surge line. Since the rationale for this scenario was as a bounding case with respect to melt stabilization and early containment pressurization, why was a larger break not analyzed?

Breaks greater than the size of the largest attached pipe result in a CDF lower than 10^{-8} . As such, they are excluded from AREVA NP's definition of a relevant scenario. In addition, MAAP4 uses a simple momentum equation which limits the ability of the code to accurately model phenomena associated with breaks as large as a double ended guillotine break. Based on these considerations, the surge line break was chosen as the bounding scenario.

- b) Following lower plenum dryout at 2 hours (Figure 7-8), there is still about 20 tons of water in the RCS. Where is this water coming from?

The additional water after lower plenum dryout is trapped in the unbroken loop intermediate leg (UIL) and broken loop intermediate leg (BIL). The location of the MAAP nodes UIL and BIL are shown in Figure RAI-46-1.

Figure RAI-46-1 MAAP4 – Primary System Water Nodes



(Reference MAAP User Manual)

- c) Is the fraction of the core/reflector in the lower plenum at the time vessel breach (see also Figure 7-11 and 7-12) a conservative estimate for melt spreading and stabilization.

The MAAP4.0.7 in-vessel core degradation modeling can be considered best estimate since the code inputs governing the in-vessel phase of the calculation have not been biased. Figures 7-11 and 7-12 display the time history of melt collection in the lower head of the RPV and the corresponding decrease in mass from the core over the course of the accident. The presence of the heavy reflector in the U.S. EPR results in a longer retention of melt in the core region so the initial melt transfer to the lower plenum is large, followed by a staged release as the failure in the heavy reflector widens and additional melt is added to the lower plenum. The release of the accumulated melt in the lower plenum in a single pour is partly the result of new modeling by FAI in MAAP4.0.7. The new modeling takes into account the effect of the outgoing melt on the RPV lower head. The additional heat flux caused by the outflowing melt on the already degraded lower vessel head causes the initial failure of the lower head to be sufficiently large to release most of the accumulated melt into the reactor pit.

- d) The MAAP analysis shows extremely efficient melt quenching evidenced by the corium temperature (Figure 7-25), and rapid containment pressurization (Figure 7-14) in about one hour. What is the modeling assumption in MAAP? Is the bottom cooling modeled?

One of the primary focuses of the improvements made in MAAP4.0.7 was to add the capability to model the cooling channels of the U.S. EPR core catcher. The cooling channels are modeled as a node in the Generalized Containment Model (GCM). Using the enhanced subroutine HTWALLN for containment heat sinks, the cooling structure was modeled as a multi-layer heat sink (sacrificial concrete and cast iron) and the cooling water starts to flow through the channels when corium arrives in the spreading room.

The heat transfer in the spreading room during core melt stabilization is a complex process with the initial phases dominated by a rapid conversion of incoming water to steam, followed by a film boiling phase with transient bulk freezing where corium fragmentation can have a noticeable effect. The analyses documented in the topical report were the first attempt by AREVA NP to model the core melt stabilization with no imposed biases in the MAAP4.0.7 modeling. These first results do not account for some uncertainties associated with the level of fragmentation and the ability of the initial incoming water to effectively cool the melt. Therefore, AREVA NP has developed a more sophisticated model of the heat transfer in the spreading area via the user-defined function feature in MAAP4.0.7 (see also RAI 27 response).

- e) In the period between about 10 and 20 hours, total containment pressure (Figure 7-14) is about 2.5 to 3.5 bar, and the average air mole fraction (Figure 7-16) is about 0.15 to 0.20, implying that the average partial pressure of air is only about 0.5 bar. Since no failure of containment was mentioned in the calculation results, where has the rest of the air gone (approximately 1.0 bar at the beginning of the scenario?)

The initial condition of the containment atmosphere contains approximately 50% relative humidity.

- f) How much time is required for the melt in the reactor cavity to reach the stabilized melt conditions that are desired prior to melt transfer? Given that calculations show about one to two hours will elapse between reactor vessel failure and melt plug failure, does an adequate margin of time exist within which to guarantee these melt conditions?

The melt conditions desired for melt transfer are dependent on the thickness and material properties of the sacrificial concrete. The thickness of sacrificial concrete required to obtain the desired melt conditions is 50 cm. The ablation rate of the sacrificial concrete will vary with decay heat and relocation speed of the melt. For a scenario where the melt has a high decay heat, the amount of time between reactor vessel failure and melt plug failure will be shorter compared to a scenario with a low decay heat. The relocation speed of the melt can increase or decrease the erosion rate of the sacrificial concrete affecting the time that elapses between vessel failure and melt plug failure. The variation in time between reactor vessel failure and melt plug failure discussed above can be seen in the event progression tables in Section 7.

RAI 47: Section 7.3.2, Figure 7-38:

What causes the reductions in hydrogen mole fractions? Burns? PAR operation? What causes the increase following vessel failure? Core debris/concrete interactions? Please provide a plot of CO mole fraction.

Response 47:

The decrease in the hydrogen mole fraction throughout the SBO scenario is attributed to the operation of the 47 PARs located throughout the containment. There are three events occurring around 4 hours, 7.3 hours, and 9 hours that result in an increase in the hydrogen mole fraction. At 4 hours, core damage occurs and significant hydrogen is generated. A release into the containment occurs because the pressurizer safety valves open to relieve the reactor coolant system from the loss of heat sink, which is a consequence of the station blackout (SBO) scenario. At 7.3 hours, the reactor pressure vessel fails resulting in relocation of the core to the reactor cavity and, subsequently, Molten Core-Concrete Interaction (MCCI). At 9 hours, the gate fails and melt is relocated to the spreading compartment. Flooding begins, resulting in a significant amount of steam being released from the spreading area compartment and pressurizing the containment. Since the mole fraction is a function of the conditions of the atmosphere (pressure, temperature, and other constituents), it reflects this event. Figure 7-41 in the topical report shows the mass of hydrogen in containment, which is not dependent on the containment conditions. Figure 7-38 in the topical report was mislabeled. In fact, it shows the mole fraction of combustible gas (both H₂ and CO). CO is a product of MCCI; hence, it appears only after reactor vessel failure, lasts only as long as corium is in contact with concrete (a few hours), and is not impacted by the H₂ recombiners. As such, the mass of CO in the containment reaches a maximum relatively quickly. The corresponding mole fraction is approximately 1%. The topical report will be revised to include the updated figures, including separate H₂ and CO mole fraction plots.

RAI 48: Appendix C:

Have any calculations been performed using the MELCOR 1.8.6 input deck described in Appendix C for U.S. EPR?

Response 48:

Concurrent with the development of the analysis capability presented in Section 6.1 of the topical report, AREVA sponsored the development of a U.S. EPR model for the MELCOR 1.8.6 code. The motivation for this work was to develop some expertise and understanding of alternative analysis approaches and evaluate the merits of a MELCOR-based U.S. EPR methodology for severe accident safety issue resolution. The development of the MELCOR model and subsequent analysis involved several technical challenges that ultimately resulted in our abandonment of this option. Considering this decision, the inclusion of Appendix C is superfluous to the objectives of the topical report. The topical will be revised to eliminate this Appendix. (See also RAI 38 response).

RAI 49: Section 2.2.2.1:

Even though the PAR units are equipped with a horizontal cover on top, aerosol-laden gases can still enter the units from the bottom, possibly depositing on the catalytic plates. Please discuss the potential for degradation of recombiner capacity under high aerosol loading conditions of severe accidents. This should include a listing of design qualification tests to support the recombination rates for the PAR units. Please discuss the potential for decomposition of iodine and other fission product aerosol compounds (e.g., CsI, AgI, etc.) within the proposed PAR units resulting in the evolution of fission products in their gaseous (more volatile) forms (e.g., I₂). Please provide information on available experimental data (prototypic of PAR conditions in U.S. EPR) that can support the discussions. PARs can also reach high enough temperatures that can potentially serve as an ignition source inside containment. Please discuss the potential consequences of PAR-induced combustion of hydrogen (and CO) as a consequence of prolonged operation of PARs. Please provide support that the PARs are qualified to withstand the temperature and pressure loads that might be expected under severe accident conditions, including hydrogen combustion, DCH, and steam explosions.

Response 49:

As noted in the topical report, the AREVA PAR design includes a horizontal housing cover at the top of the recombiner to protect the catalyst against direct spray of water and aerosol deposition. In addition, numerous parallel plates with a catalytically active coating are arranged vertically in the bottom of the housing providing a torturous path for potential aerosol contaminants. The AREVA PAR design has undergone an extensive testing program as part of qualification efforts for European authorities. Both the KALI and H2PAR programs specifically featured this design in the execution of tests examining PAR performance under the atmospheric, event, and poison uncertainties identified in Table RAI-49-1. The KALI program focused primarily on a wide range of hydrogen concentrations, initial ambient gas temperatures and pressures, steam and nitrogen as inert gases, and potential poisons. In addition, the effects of wetness and low ambient temperature on PAR start-up were studied. The H2-PAR test program is considered the most important test program concerning poisoning, deposition and contamination of catalyst in a post accident atmosphere. During this program, the AREVA PAR was subjected to a realistic aerosol exposure generated by a molten core. These tests were designed to address the question of the effect of aerosols on the catalytic recombination as well as the catalytic poisoning by fission products in a severe accident atmosphere. The

principal conclusion from these tests was that no significant reduction in performance was observed.

While AREVA considers the specifics describing the performance of the PARs under adverse conditions to be a design certification issue outside the scope of this topical, PAR performance uncertainties are examined as part of analytical studies supporting safety issue resolution. RAI 43 response details further information on this subject.

Table RAI-49-1 Conditions Examined During PAR Testing

<u>Atmospheric Dependencies</u>	<u>Event Dependencies</u>	<u>Poison Dependencies</u>
H ₂ - Concentration	Cable Fire/ degradation	Iodine
Temperature	Oil Fire	Organic Iodine
Pressure	Water submergence	Tellurium
Steam/Humidity Inerting	Blow Down Test	Selenium
Influence of Low Oxygen	Operational vibrations	Antimony
Spray-System operation	Seismic Vibrations	Fission Products
Recombiner arrangement in Multi- compartment geometry	Function after H ₂ -Deflagration	Aerosol exposure
Influence of CO	Ignition/Deflagration investigation	Welding fume test
		Solvent fume test